

AD720404

SEMI-ANNUAL TECHNICAL STATUS REPORT

ON

MOLECULAR LASER STUDY

3-5 MICRONS

August 1, 1970 Thru January 1, 1971

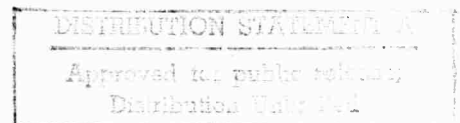
Prepared by  
Bernard G. Huth  
Principal Investigator  
IBM  
Federal Systems Division  
Gaithersburg, Maryland 20760  
301/840-6941



Contract No. N00014-71-C-0010  
Sponsored by  
ADVANCED RESEARCH PROJECTS AGENCY  
ARPA Order No. 306  
Program Code No. 421

Effective Date: August 1, 1970  
Expiration Date: July 31, 1971  
\$49,980

Scientific Officer: Director, Physics Programs  
Physical Sciences Division  
Office of Naval Research  
Department of the Navy  
Arlington, Virginia 22217



The views and conclusions contained in this document are those of the authors and should not be interpreted as necessarily representing the official policies, either expressed or implied, of the Advanced Research Projects Agency or the U. S. Government.

Details of illustrations in  
this document may be better  
studied on microfiche

Reproduced by  
NATIONAL TECHNICAL  
INFORMATION SERVICE  
Springfield, Va. 22151

37

## 1.0 INTRODUCTION

This first Semi-Annual Technical Report is in partial fulfillment of the contract requirements as specified in the Contract Schedule, Section 6, Paragraph I(B).

Since this is the first technical report written on this contract, it will also present some pertinent background on molecular lasers. This will be in the form of a brief review of  $N_2-CO_2-He$  lasers and the operation of our plasma tubes, to be presented in Section 2.0. Discussion of laser emission from a mixture of  $H_2-C_2H_2-He$  will be presented in Section

Section 4.0 will outline the proposed experimental work to be carried out in the second half of the contract period.

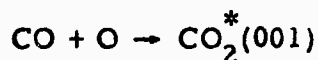
The operation of the first acetylene laser and identification of the lasing transition were carried out by Dr. Carl F. Shelton. He initiated the experimental program at IBM and was the Principal Investigator for the first quarter of the performance period for this contract.

## 2.0 BRIEF REVIEW OF N<sub>2</sub>-CO<sub>2</sub>-He LASERS

The pumping mechanisms and operation of the N<sub>2</sub>-CO<sub>2</sub>-He laser system have been widely discussed in the open literature and thus will only be summarized briefly here.

Excitation mechanisms for pumping CO<sub>2</sub> to the upper laser level include:

- (a) Direct electron impact<sup>(1)</sup>,
- (b) Vibrational energy transfer<sup>(2)</sup> through inelastic collisions with N<sub>2</sub><sup>\*</sup>(v = 1),
- (c) Recombinations<sup>(3)</sup> of the form



Helium enhances the CO<sub>2</sub> laser output by at least five mechanisms:

- (1) Helium depopulates the 01<sup>1</sup>0 mode through inelastic collisions and thus indirectly increases the rate of depopulation of the lower laser level, i. e., the 10<sup>0</sup>0 level<sup>(4)</sup>.
- (2) Helium increases the rate of rotational thermalization within each vibrational level and thus maintains the population inversion on the strongest vibrational-rotational transitions.
- (3) Helium cools the kinetic temperature of the gas mixture because of its higher thermal conductivity.
- (4) Helium shifts the electron temperature and/or the electron density to more favorable values for vibrational excitation by electron impact<sup>(4, 5)</sup>.
- (5) Helium reduces the diffusion of the excited species to the walls of the plasma tube where they can be de-excited.

Effect (2) shows up in the fact that fewer rotational P-branch lines are observed in N<sub>2</sub>-CO<sub>2</sub>-He mixtures than in N<sub>2</sub>-CO<sub>2</sub> mixtures. Patel<sup>(3)</sup> observed emission on the P(12) through P(38) lines of the ν<sub>3</sub> - ν<sub>1</sub> band with pure CO<sub>2</sub>. Other researchers have observed emission on the P(18) through P(28) lines using

$N_2$ - $CO_2$ <sup>(6)</sup>, the P(20) through P(26) lines using  $CO_2$ -He<sup>(7)</sup> and the P(20) through P(24) using  $N_2$ - $CO_2$ -He<sup>(8)</sup>. Again, since only the even P-branch lines are allowed this means a reduction from fourteen lines using pure  $CO_2$  to four lines using  $CO_2$ -He and to three lines using  $N_2$ - $CO_2$ -He.

The actual effects of He on electron temperature and electron density in the plasma have not been accurately measured during laser emission, however, these effects can be inferred in various ways. Patel<sup>(9)</sup>, for example, observed an increase in output from his parallel pumped  $N_2$ - $CO_2$  laser<sup>(10)</sup> with increasing helium partial pressure when the helium was added through the  $CO_2$  port and  $CO_2$ -He mixed with the vibrationally excited  $N_2$  in the interaction region. An even greater increase in power output, by roughly a factor of two, was observed by Patel when the helium was added through the  $N_2$  port and was thus in the parallel discharge with the  $N_2$  prior to mixing with  $CO_2$  in the interaction region. This same effect has been observed with a parallel-pumped tube built at IBM and shown in Figure 3.

The electron-energy distribution in the positive column of a normal glow discharge is controlled in part by the ionization potentials of the components of the gas mixture. The trend is to a higher electron temperature with higher ionization potentials<sup>(4,11)</sup>. The ionization potentials of  $N_2$ ,  $CO_2$  and He are 15.5, 13.79 and 24.58ev, respectively. Typical mixtures used for laser emission vary, but a mixture of 2/1/10,  $N_2/CO_2/He$  is not uncommon.

Thus, there is some evidence that one of the significant roles played by helium in  $N_2$ - $CO_2$ -He lasers is to shift the electron temperature to a slightly higher value for a given total pressure and thus increase the pumping of the upper laser level by direct electron impact and by vibrational energy transfer from  $N_2^*(v=1)$ .

The pulsed plasma tube used for most of the  $H_2$ - $C_2H_2$ -He work is straightforward and is shown in Figure 1. The mirrors are exposed to the vacuum, and are mounted by means of stainless steel bellows. Operation of the tube with  $N_2$ - $CO_2$ -He is indicated in Figure 2. The ratio of  $N_2:CO_2:He$  used for the data shown was 2:1:4 at 8 Torr and produced pulse energies of 15 to 20 millijoules.

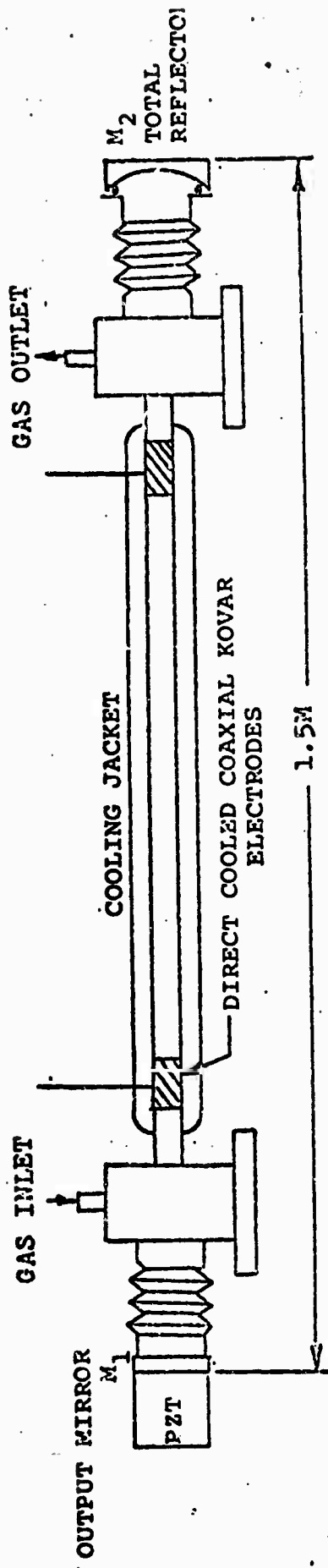
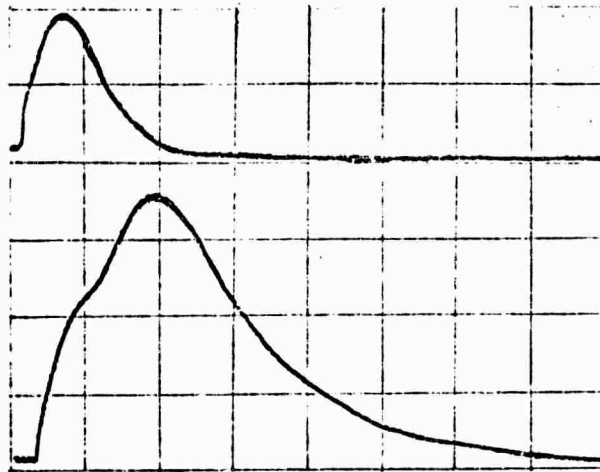


Figure 1. Pulsed Excitation Plasma Tube with Coaxial Kovar Electrodes.

N<sub>2</sub>-CO<sub>2</sub>-He

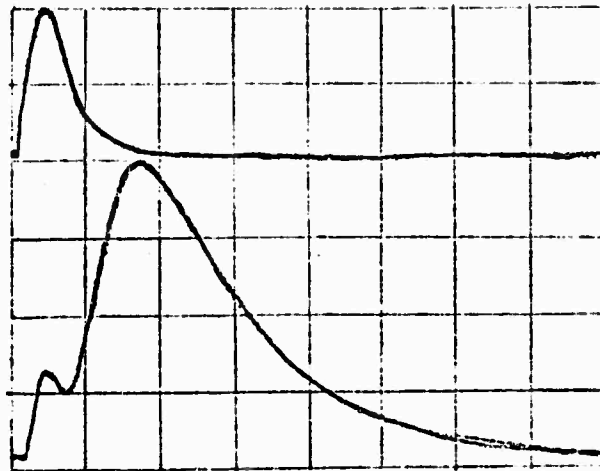
100 MA/DIV



CURRENT

LASER

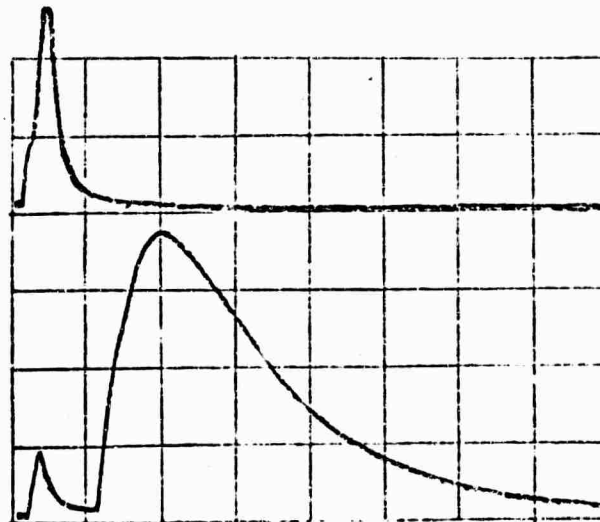
200 MA/DIV



CURRENT

LASER

500 MA/DIV



CURRENT

LASER

200 USEC/DIV

Figure 2

2-4

57.1% He  
28.6% N<sub>2</sub>  
14.3% CO<sub>2</sub>  
P = 8 Torr

The parallel tube shown in Figure 3 produced CW power outputs in excess of 600mW from  $\text{CO}_2$  which had been pumped only from a resonant energy transfer from  $\text{N}_2$  which was excited in the parallel discharge. For these experiments a 95% reflectivity dielectric mirror was used for output coupling, and an input power of 220 watts was used. This compares to an output power of the order of 2mW with an input power of 100 watts obtained by Patel<sup>(5)</sup>.

This parallel tube was also operated in the pulsed mode by the addition of two electrodes near the center of the discharge region to prevent the plasma from traveling down the interaction region. Figure 4 shows a diagram of the modified tube and the pulse circuitry.

A 0-16Kv, 0-12ma dc power supply was used to charge a 0.02uf capacitor. This charge was then applied to the plasma tube when the electrode shown on the right in Figure 4 was switched to ground by the thyatron tube. The pulse repetition rate could be controlled by a pulse generator which triggered the thyatron. Two Welch Model 1397, 15cfm each, mechanical pumps were operated in parallel in order to continuously flow gas mixtures through the plasma tube. Partial pressures and flow rates of up to three component gases could be controlled through the use of needle valves, flow meters and a manifold arrangement. Partial pressures were measured upstream of the plasma tube using a capacitor manometer.

Figure 5 shows the performance of this tube with  $\text{CO}_2$  under pulsed conditions. Output pulse energies were typically 3 millijoules, and the peak power was approximately 7 watts. The nitrogen flow rate was approximately 60 liters/min at the tube which produced a flow velocity of 400cm/sec in each half of the interaction region. Morgan and Shiff have measured the lifetime of the metastable  $\text{N}_2^*(v=1)$  level at a few Torr to be 114msec, which means that if wall collisions are unimportant, the excited molecules travel 45cm in one decay time. Considering both halves of the tube, this represents almost the entire 1 meter length of the interaction region.

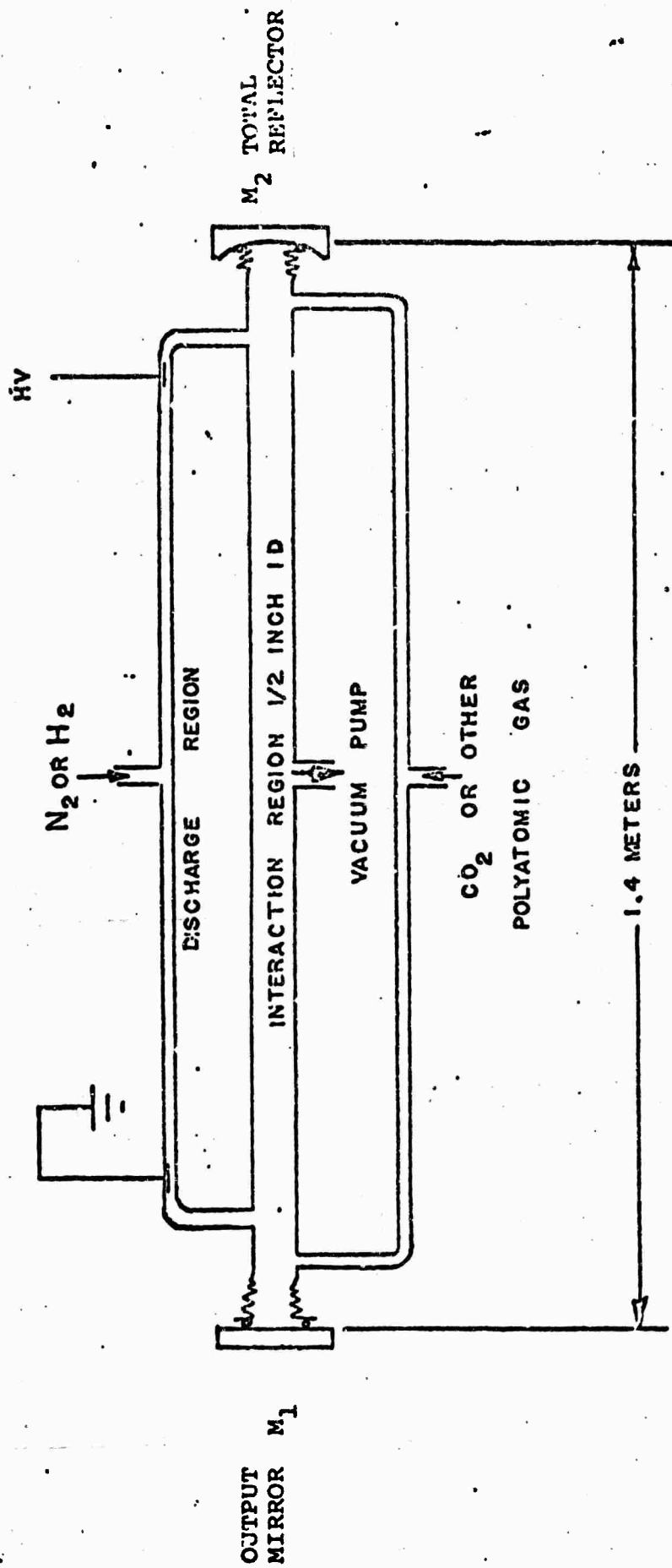


Figure 3. Parallel Tube



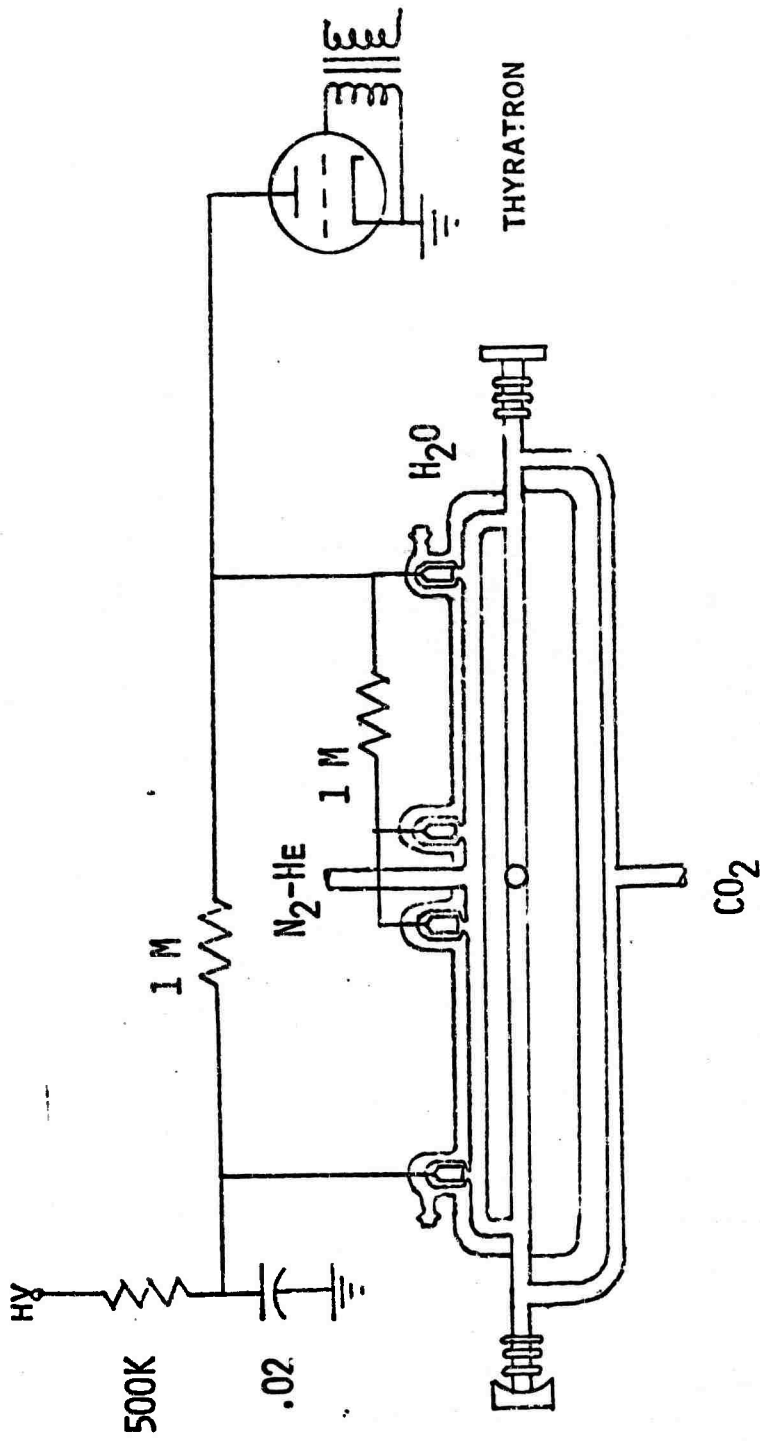
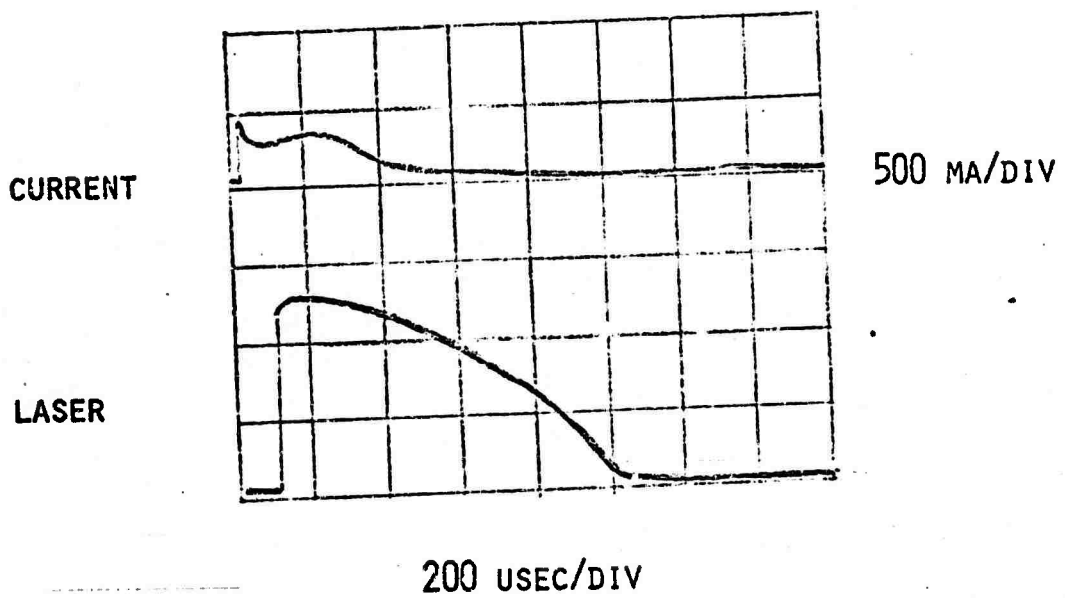


DIAGRAM OF PULSED PARALLEL TUBE

Figure 4



PULSED  $N_2-CO_2-He$  IN PARALLEL TUBE

Figure 5

### 3.0 STIMULATED EMISSION FROM $H_2-C_2H_2-He$

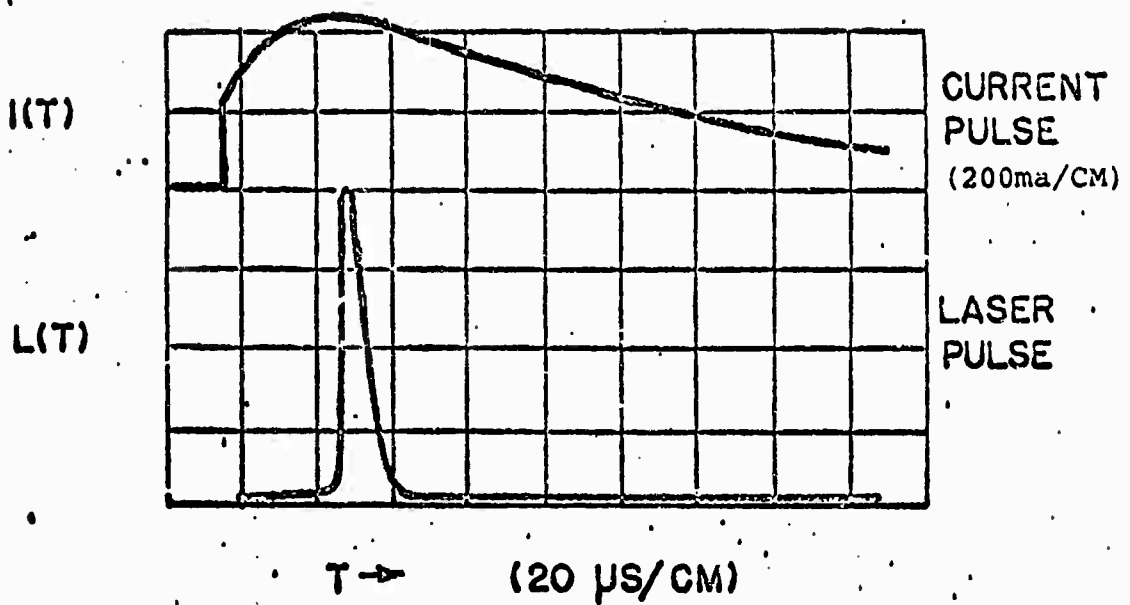
Laser emission near 8 microns has been obtained from a flowing mixture of  $H_2-C_2H_2-He$  under pulsed excitation conditions in a gas discharge<sup>(12,13)</sup>. This lasing action may result from vibrational excitation of  $C_2H_2$  via a near resonant energy transfer from the metastable  $v = 1$  vibrational level of  $H_2$  which has been excited in the helium rich discharge as well as possible direct electron impact excitation of  $C_2H_2$ . Laser action has been observed, however, without the presence of hydrogen in the discharge.

A Jarrell-Ash one-meter Czerny-Turner spectrometer with a 98 groove/mm IR grating, blazed at  $7\mu$  was used to measure the wavelength of the laser emission. This grating gave a linear dispersion of approximately 102Å/mm and a theoretical resolving power of 8Å in the first order. The precision of the wavelength counter is  $\pm 1\text{Å}$  with a 1180 groove/mm grating. This corresponds to a precision of  $\pm 12\text{Å}$  with the 98 groove/mm grating. A liquid nitrogen cooled Ge: Au detector was used in these experiments. This detector has a specified time response of 20ns

### 3.1 $H_2-C_2H_2-He$ LASER CHARACTERISTICS

Representative results with the pulsed tube in Figure 1 showing the current pulse through the  $H_2-C_2H_2-He$  plasma and the laser pulse obtained are shown in Figures 6 and 7. A flowing mixture of approximately 1 torr  $C_2H_2$ , 2 torr  $H_2$  and 20 torr He was used in each case. The values of peak powers given were measured with no attempt being made to optimize the output coupling.

The first results were obtained using an aperture for broadband output coupling and is shown in Figure 6. The laser emission was usually found to be on a single line at  $8.040\mu$  and no rotational structure was observed. However,



$M_1$ : Flat Au-coated  $BaF_2$  with 1/2 mm dia. hole

$M_2$ : R=5 meters Au-coated

$H_2/C_2H_2/He=2/1/20$  torr

$T_{jacket}=22^{\circ}C$ .

1/2 inch ID Plasma tube with neon sign electrodes

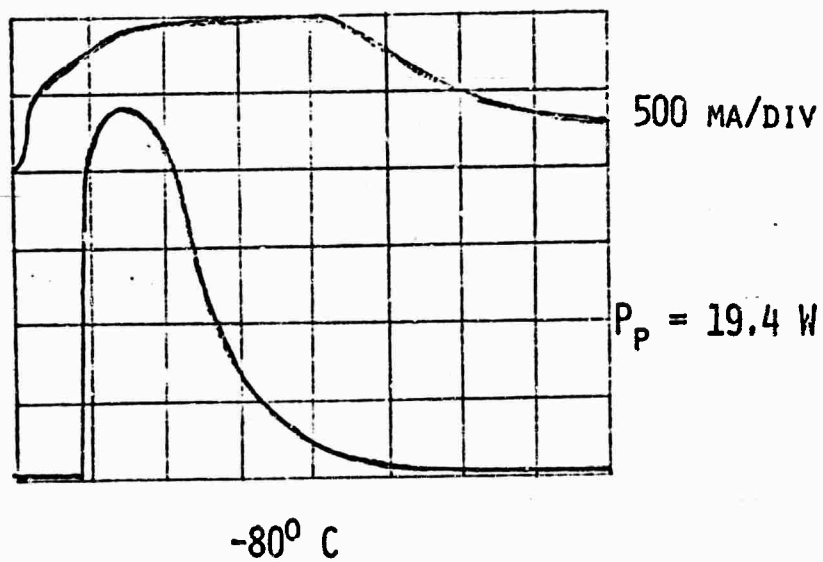
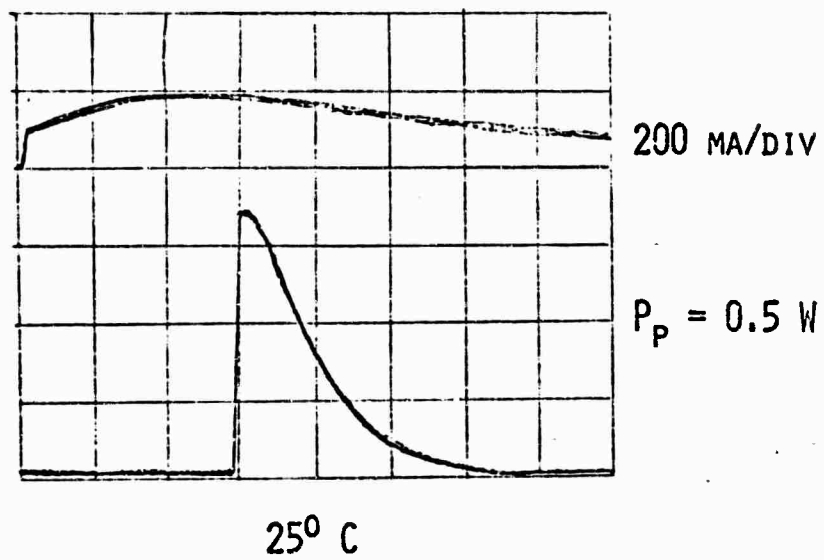
Peak power = 5.7 watts

PRF = 32 pulses/sec

Figure 6. First Laser Output Obtained from  $H_2-C_2H_2-He$  Mixture.

H<sub>2</sub>-C<sub>2</sub>H<sub>2</sub>-He

2:1 20 Torr



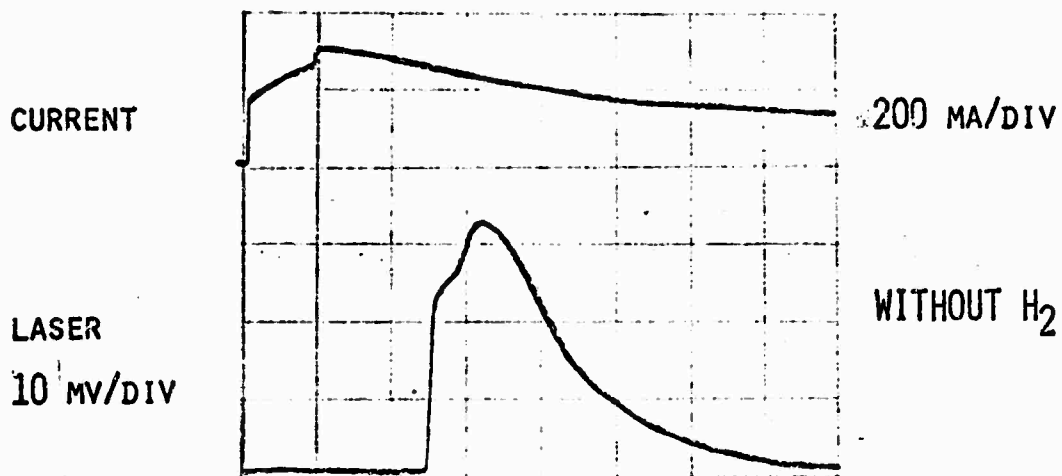
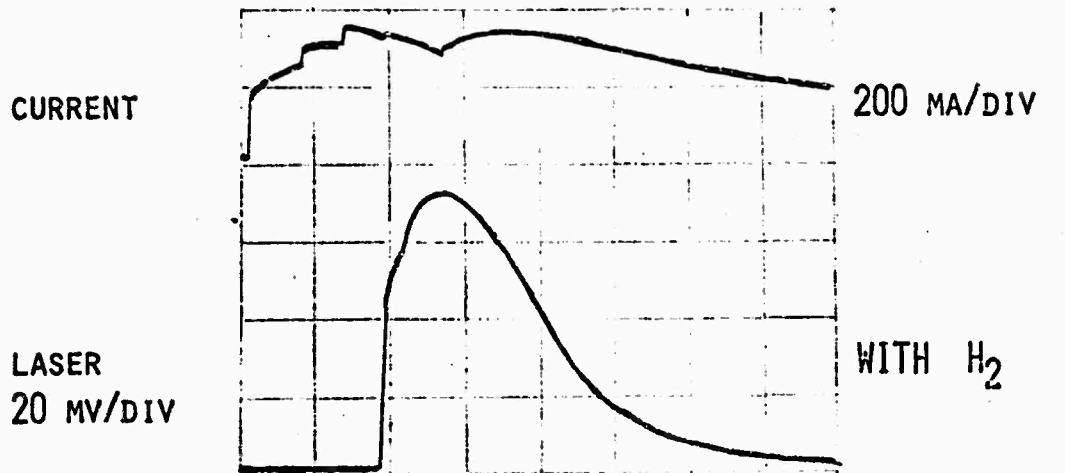
2:1:23 Torr

Figure 7

on one occasion, two lines were observed at 8.034  $\mu$  and at 8.040  $\mu$ .

The results obtained using narrow band dielectric mirrors are shown in Figure 7. The laser pulses shown are for two cooling jacket temperatures. Figure 7b shows the result obtained when the gas mixture was pre-cooled and the cooling jacket temperature was  $-80^{\circ}\text{C}$ . Five emission lines were observed at different times under these conditions. The wavelengths in air of these five lines were measured as 8.0313, 8.0329, 8.0352, 8.0383 and 8.0416  $\mu$  using the 12th order of the 6678 $\text{\AA}$  and 6717 $\text{\AA}$  neon lines as a calibration reference. The accuracy of these wavelength measurements was probably better than  $\pm 2\text{\AA}$ . A 40:1 increase in peak power was observed in cooling the discharge from  $22^{\circ}\text{C}$  to  $-80^{\circ}\text{C}$  as noted in Figure 7.

Laser action in  $\text{H}_2\text{-C}_2\text{H}_2\text{-He}$  in the 1/2 inch I.D. plasma tube could only be obtained over a very narrow range of discharge conditions, i. e., discharge current, and over a very narrow range of gas mixtures. Laser emission was not observed from a pure  $\text{C}_2\text{H}_2$  plasma or a  $\text{C}_2\text{H}_2\text{-H}_2$  plasma, but it was observed with a  $\text{C}_2\text{H}_2\text{-He}$  plasma. Figure 8 shows the results when the hydrogen was removed from the discharge. In the upper curve, the pressures of  $\text{H}_2\text{-C}_2\text{H}_2\text{-He}$  were 2, 1, and 32 torr, respectively, and in the lower curve the pressures were 0, 1, 32 torr. In both cases, both the gas and cooling jacket were at  $-60^{\circ}\text{C}$ . Without hydrogen, the peak power was reduced by a factor of 2, and the pulse energy was reduced even more because of the slight decrease in pulse width. The same spectral lines were observed in the laser output both with and without hydrogen.



20 USEC/DIV

OPERATION WITHOUT HYDROGEN

Figure 8

Lasing again with reduced output occurred when  $N_2$  was substituted for  $H_2$ . In this case an increasing delay time ranging from 20 to 65 usec accompanied the decreasing output.

These last results indicate that either some species other than  $C_2H_2$  may be producing the laser emission or that direct electron impact excitation of  $C_2H_2$  can alone lead to laser emission. They do not, however, completely rule out resonant energy transfer from  $H_2^*(v = 1)$  as a possible pumping mechanism.

These results further support the fact that much work is needed in understanding the complex discharge chemistry and various pumping mechanisms involved as discussed in Section 3.3.

Laser emission was obtained at pulse repetition rates from 1pps up to 250 pps. Power supply limitations, i. e., current capability, prevented operation at higher repetition rates. The discharge ran quite clean, although light carbon deposits were formed near the electrodes after many hours of operation at pulse repetition rates of the order of 26pps. The side light emission from the plasma was very weak during laser action and, in fact, could not be observed with the eye when the laboratory lights were turned on.

### 3.2 POSSIBLE IDENTIFICATION OF LASER TRANSITIONS

Acetylene,  $C_2H_2$ , is a linear symmetric molecule with five normal modes of vibration<sup>(14)</sup>. These normal modes are shown in Figure 9. Some of the vibrational energy levels of the ground electronic state of  $C_2H_2$  are shown in Figure 10. In contrast to the  $\nu_3 - \nu_1$  band of  $CO_2$ , the  $\nu_2 - \nu_5^1$  ( $01000 - 00001^0$ ) band of  $C_2H_2$  has an allowed Q-branch<sup>(14)</sup>. This  $\nu_2 - \nu_5^1$  band Q-branch has been observed in absorption by Bell and Nielsen<sup>(24,25)</sup> with



$C_2H_2$  - ACETYLENE  
 Linear Symmetric Molecule  
 $H-C\equiv C-H$

<u>NORMAL MODE</u>		<u>ASSIGNMENT</u>
$v_1$		$\Sigma_g^+$
$v_2$		$\Sigma_g^+$
$v_3$		$\Sigma_u^+$
$v_4$		$\Pi_g$
$v_5$		$\Pi_u$

Figure 9. Normal Vibrational Modes of Acetylene

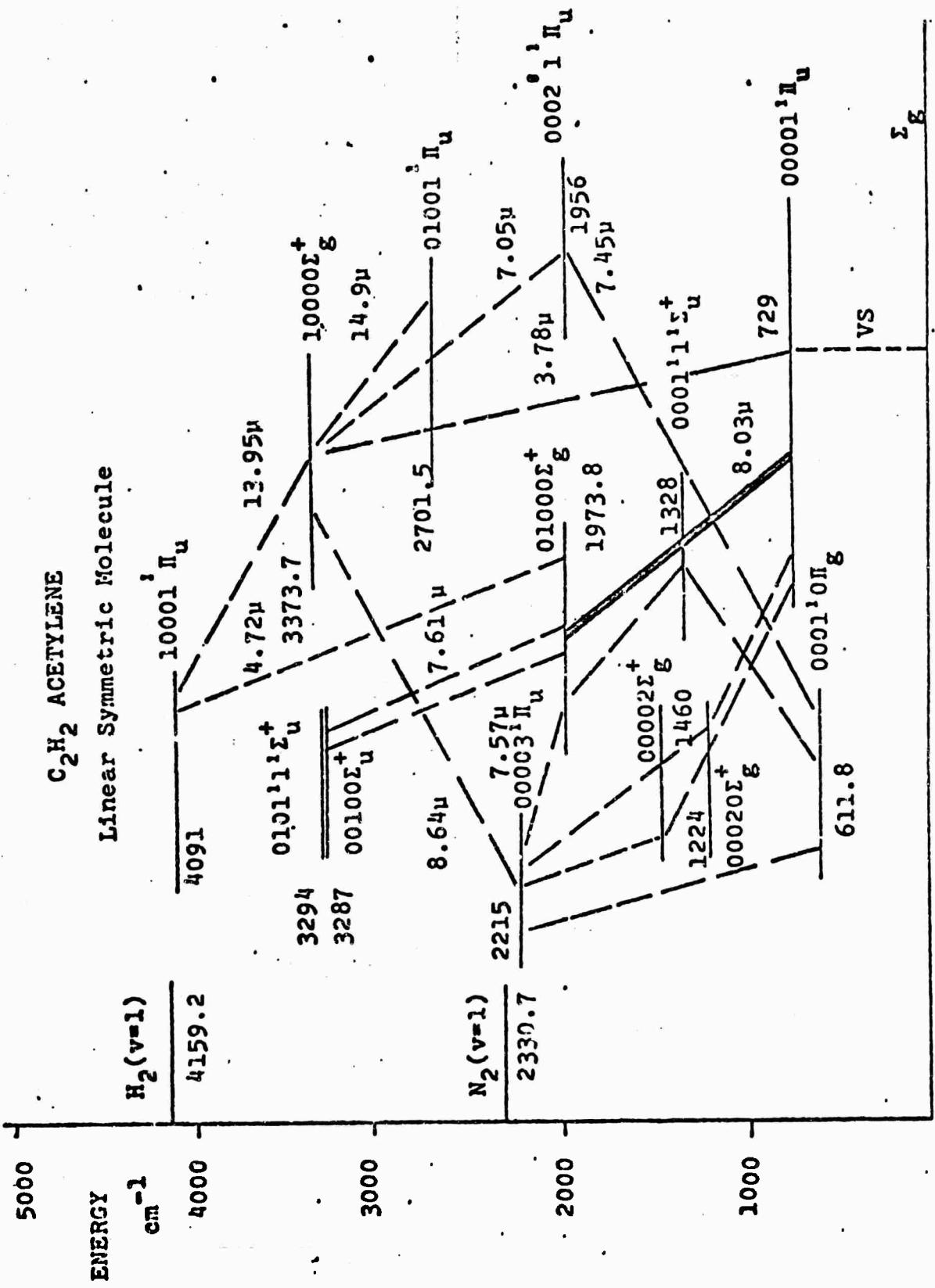


Figure 10. Vibrational Energy Level Diagram of Acetylene

Thus, equation (3-3) can be written as

$$Q(J) = \nu_0' + (B_U - B_L)J(J+1) + \dots \quad (3-4a)$$

This equation can be used to calculate the energies of the Q-branch lines of the  $\nu_2 - \nu_5^1$  band of  $C_2H_2$ . The results obtained using Herzberg's<sup>(14)</sup> values of  $B_e$ , and the  $\alpha_i$ 's,

$$B_e = 1.1838\text{cm}^{-1}$$

$$\nu_0' = 1245.28\text{cm}^{-1} *$$

$$\alpha_1 = 0.008\text{cm}^{-1}$$

$$\alpha_2 = 0.0063\text{cm}^{-1}$$

$$\alpha_3 = 0.0056\text{cm}^{-1}$$

$$\alpha_4 = -0.0013\text{cm}^{-1}$$

$$\alpha_5 = -0.0022\text{cm}^{-1}$$

giving,

$$B_U = B_{\nu_2} = 1.17105\text{cm}^{-1}$$

$$B_L = B_{\nu_5^1} = 1.17955\text{cm}^{-1}$$

$$\text{or, } \Delta B = B_U - B_L = -0.00850\text{cm}^{-1}$$

are shown in Table 1 for the first twenty Q-branch transitions of the  $\nu_2 - \nu_5^1$  band of  $C_2H_2$ . Normally, for the  $C_2H_2$  the lines with odd J should be more intense than the even J due to the 3:1 ratio of the statistical weights<sup>(14)</sup>.

---

\* Herzberg gives a value for  $\nu_0' = 1244.7\text{cm}^{-1}$ . We have adjusted this value by  $0.58\text{cm}^{-1}$  to give a better fit to the experimentally determined wavelengths.

TABLE I

Q-Branch Lines of the  $\nu_2 - \nu_5'$  Band of  $C_2H_2$  Calculated from  
 Herzberg's Data

<u>J</u>	<u><math>\Delta E</math></u>	<u><math>\lambda_{calc.}</math></u>	<u><math>\lambda_{obs.}</math></u>
1	1245.26	8.0282	
2	1245.23	8.0285	
3	1245.18	8.0288	
4	1245.11	8.0292	
5	1245.03	8.0298	
6	1244.92	8.0304	
7	1244.80	8.0312	8.0313*
8	1244.67	8.0321	
9	1244.52	8.0331	8.0329
10	1244.35	8.0342	
11	1244.16	8.0354	8.0352
12	1243.95	8.0367	
13	1243.73	8.0381	8.0383
14	1243.50	8.0397	
15	1243.24	8.0413	8.0416
16	1242.97	8.0431	
17	1242.68	8.0449	
18	1242.37	8.0469	
19	1242.05	8.0490	
20	1241.71	8.0512	

\*This line observed only once.

The results obtained Keller's<sup>(15)</sup> values of  $B_e$ , and the  $\alpha_i$ 's,

$$B_e = 1.1845\text{cm}^{-1}$$

$$\nu'_0 = 1245.20\text{cm}^{-1} **$$

$$\alpha_1 = 0.0063\text{cm}^{-1}$$

$$\alpha_2 = 0.0092\text{cm}^{-1}$$

$$\alpha_3 = 0.0053\text{cm}^{-1}$$

$$\alpha_4 = 0.00065\text{cm}^{-1}$$

$$\alpha_5 = 0.0021\text{cm}^{-1}$$

giving,

$$B_U = 1.1673\text{cm}^{-1}$$

$$B_L = 1.1786\text{cm}^{-1}$$

or,

$$B = B_U - B_L = -0.0113\text{cm}^{-1}$$

are shown in Table 2 for the first twenty Q-branch transitions of the  $\nu_2 - \nu_5^1$  band of  $C_2H_2$ . All values of  $\Delta E$  are given for vacuum and wavelengths are given in air.

---

\*\* Keller's value for  $\nu'_0 = 1244.79\text{cm}^{-1}$  which is an adjustment of  $0.41\text{cm}^{-1}$ .

TABLE 2

Q-Branch Lines of the  $\nu_2 - \nu_5$  Band of  $C_2H_2$  Calculated from  
Keller's Data

<u>J</u>	<u><math>\Delta E</math></u>	<u><math>\lambda</math> calc.</u>	<u><math>\lambda</math> obs.</u>
1	1245.18	8.0288	
2	1245.13	8.0291	
3	1245.06	8.0295	
4	1244.97	8.0301	
5	1244.86	8.0308	8.0313*
6	1244.73	8.0318	
7	1244.57	8.0327	8.0329
8	1244.39	8.0339	
9	1244.18	8.0352	8.0352
10	1243.96	8.0367	
11	1243.71	8.0385	8.0383
12	1243.44	8.0400	
13	1243.14	8.0419	8.0416
14	1243.82	8.0440	
15	1242.49	8.0462	
16	1242.13	8.0485	
17	1241.74	8.0510	
18	1241.34	8.0536	
19	1240.91	8.0564	
20	1240.45	8.0594	

\*This line only observed once.

A piezoelectric drive was used to scan one laser mirror in order to average the pulling effects and assure mode coincidence with any rotational line having sufficient gain to lase. An indication of these effects are that while operating the drive we have seldom found that a rotational line is missing. This is commonly the case with a fixed cavity length. Thus, scanning the cavity provides the best (unshifted) lasing spectrum available.

Phase sensitive synchronous amplification of a Ge: Au detector output was used; the amplifier gives a dc output proportional to the laser emission which is used as input to the Y-channel of an X-Y recorder. A potentiometer mounted to the wavelength drive of the spectrometer gave a dc voltage proportional to the wavelength which then drives the X-channel of the recorder. An additional moveable mirror and an S-1 PMT is used to enable the 12th order of the Ne calibration lines to be recorded on the X-Y recorder along with the  $C_2H_2$  laser lines. In all cases, dielectric mirrors were used. The total reflector has a 5 meter radius and a reflectivity of  $99.5\% \pm 0.5\%$  at 8  $\mu$ . The output mirror is flat with a reflectivity of  $98\% \pm 5\%$  at 8  $\mu$ .

Figure 11 shows a typical spectrum, and, in addition, shows the calculated wavelength of the rotational lines in the Q-branch for the rotational constants of Herzberg<sup>(14)</sup> and Keller<sup>(15)</sup>. The best fit is seen using the rotational constants of Keller. Although this fit is quite reasonable, all doubts about the identification of the transition should be removed by additional experiments, on absorption in  $C_2H_2$  planned for the third quarter.

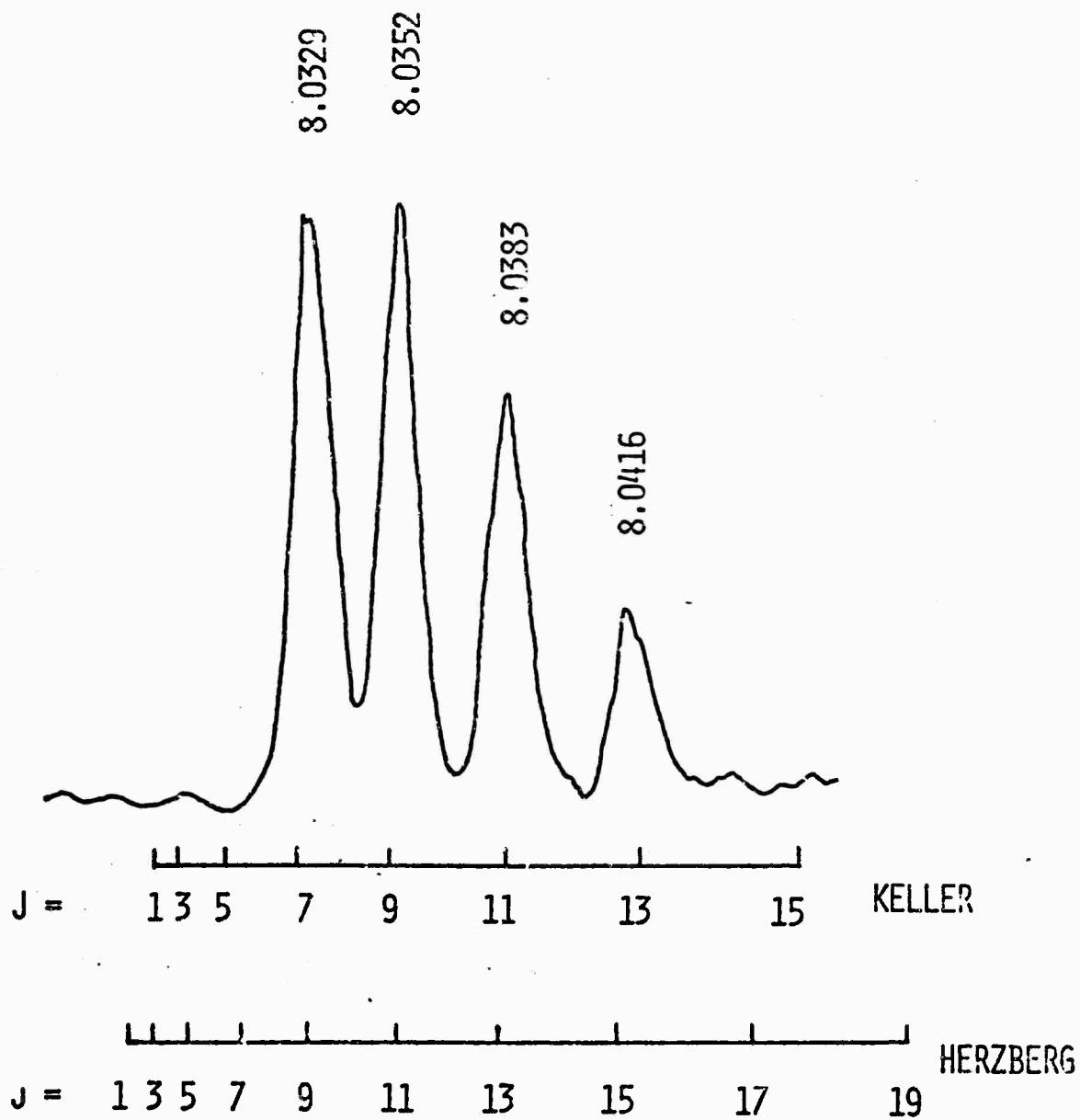


Figure 11



It is also possible that the laser emission is originating from transitions in some other species which is a dissociative product of the discharge. The carbon formation around the electrodes indicates that some dissociation of the  $C_2H_2$  is occurring to form free carbon. The dissociation energies of  $C_2H_2$  are given by Lathan, et al<sup>(23)</sup>. The pertinent reactions are



These values are the same order of magnitude as the  $CO_2 \rightarrow CO + O$  band strength at 5.6ev. Thus, there are certainly many dissociative products of  $C_2H_2$  in the discharge.

An observation of the visible spectrum of the discharge showed fairly weak CH lines,  $C_2$  Swan bands,  $H_\beta$  and He emission lines. None of these observed bands or lines are very strong, including the  $C_2$  bands, indicating that the dissociation was not appreciable.

Ethylene,  $C_2H_4$ , and ethane,  $C_2H_6$ , could also be formed in the discharge through hydrogenation of  $C_2H_2$ .



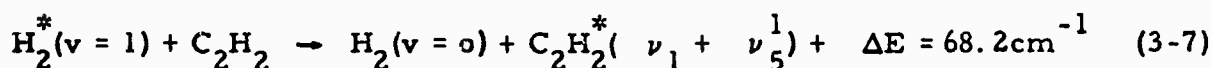
It is also possible that formation of diacetylene,  $C_4H_2$ , can occur.

Thus, possible constituents of the plasma include  $C_2H_2$ ,  $C_2H_4$ ,  $C_2H_6$ ,  $C_4H_2$ , CH,  $CH_2$ ,  $CH_3$  and  $C_2H_5$  as well as ions of these species and the laser emission may be originating from one of these.

The observation of only five emission lines from the laser, probably due to rapid rotational thermalization caused by the high helium content of the plasma, makes a positive identification of the laser transitions from rotational structure difficult.

### 3.3 DISCUSSION OF POSSIBLE PUMPING MECHANISMS

Assuming that the laser emission is occurring on Q-branch transitions of the  $C_2H_2$   $\nu_2 - \nu_5^1$  band, the laser would then be functioning as a classical four level laser (refer again to Figure 10). Two possible pumping mechanisms for obtaining population inversion in  $C_2H_2$  are direct electron impact excitation and a near resonant vibrational energy transfer from the  $H_2^*(v = 1)$  which has been excited by electron impact in the helium rich plasma.



The excited state produced by the inelastic collision process shown in Equation (4-5) is not indicated since the details of this process are now known at this time, nor is the relative importance of this mechanism in pumping  $C_2H_2$  known. The  $C_2H_2^*(\nu_1 + \nu_5^1)$  level on the right-hand side of process (3-7) can cascade via collisions or radiative transitions to the  $\nu_2$  level, which is the upper laser level. The lower laser level, the  $\nu_5^1$  level, can be de-populated through the strongly allowed  $\nu_5^1$  to the ground vibration level transition.

Vibrationally excited, ground-electronic-state hydrogen molecules have been observed as a long-lived product of a microwave discharge in pure hydrogen gas by Heidner and Kasper<sup>(16)</sup>. These excited molecules were identified by their vacuum-ultraviolet absorption spectrum. They concluded that,

at a pressure of 3 torr, hydrogen passed through a microwave discharge contains approximately 1-4% of the molecules in the  $v'' = 1$  state 25msec after leaving the discharge. This compares with 30% of the  $N_2$  molecules in the  $v'' = 1$  state in a low pressure microwave discharge in pure  $N_2$  as determined by Kaufman and Kelso<sup>(17)</sup>.

The relaxation time of the  $H_2^*(v = 1)$  level should be about 250msec at  $T = 300^\circ K$  and  $p = 3$  torr<sup>(16, 18)</sup>. This compares to the relaxation time of 114msec of  $N_2^*(v = 1)$  at  $T = 300^\circ K$  and pressures of the order of a few torr as determined by Morgan and Schiff<sup>(24)</sup>.

The cross section as a function of electron energy,  $\sigma(E)$  for the process (3-6) has been measured by Schulz<sup>(19)</sup>. It has a peak value of  $0.55 \times 10^{-16} \text{ cm}^2$  at 2.2eV compared to a peak value of  $1.5 \times 10^{-16} \text{ cm}^2$  at 2.2eV for the vibrational excitation of  $N_2$  by direct electron impact. From  $\sigma(E)$ , the rate coefficient for the excitation of  $H_2$  by direct electron impact can be calculated<sup>(20)</sup>.

$$X(t) = N_e(t) \langle \sigma v \rangle \quad (3-8)$$

where  $N_e(t)$  is the electron density in the plasma and  $\langle \sigma v \rangle$  is Schulz's cross section averaged over the electron velocity distribution in the plasma. Assuming a Maxwellian energy distribution for the electron in the plasma,

$$\langle \sigma v \rangle = K_0 T_e^{-3/2} \int E \sigma(E) e^{-E/T_e} dE \quad (3-9)$$

where  $K_0 = 6.6971 \times 10^7$  and  $T_e$  is the average electron temperature in eV. The term  $\langle \sigma v \rangle$  given by Equation (3-9) is plotted versus electron temperature in Figure 12. It is clear from Equations (3-8) and (3-9) and from Figure 12

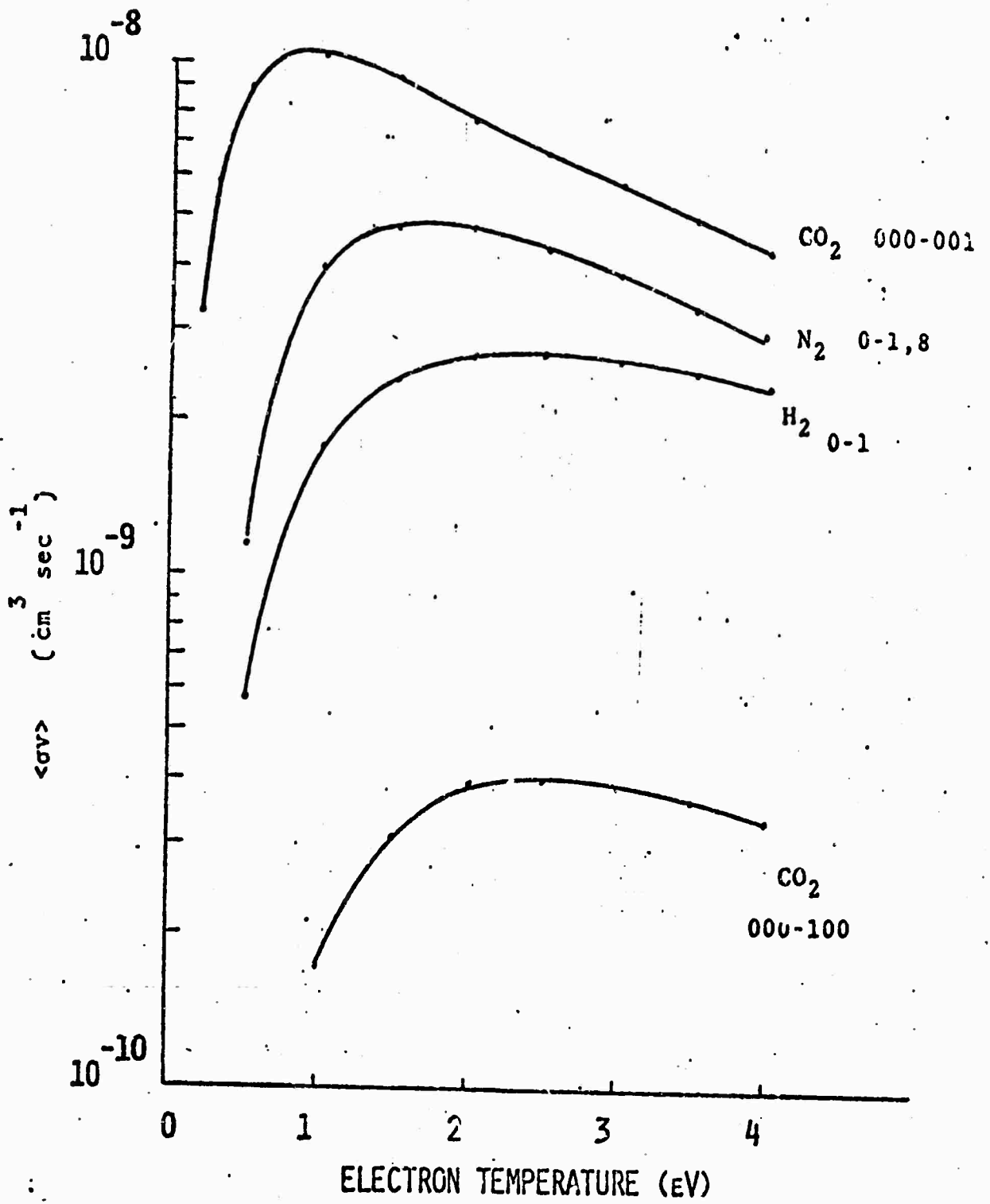


Figure 12.  $\langle \sigma v \rangle$  vs. Electron Temperature

that the rate coefficient for vibrational excitation of  $H_2$  by direct electron impact depends both upon the electron temperature and the electron density in the plasma.

Data is available in the literature on the electron temperature in pure gases under normal glow discharge conditions, but very little data is available for gas mixtures. The electron temperature,  $T_e$ , as a function of ionization potential,  $u_i$ , pressure,  $p$ , and tube radius,  $R$ , and an empirical constant,  $c$ , which depends on the gas, is given by Brown<sup>(11)</sup> (see also von Engel<sup>(12)</sup>, pages 63 and 242).

$$\left(\frac{U_i}{T_e}\right)^{-1/2} \exp\left\{\frac{U_i}{T_e}\right\} = 1.16 \times 10^7 c^2 p^2 R^2 \quad (3-10)$$

The derivation of this equation is also presented in Reference 12. The electron temperature versus pressure in the positive column of a low pressure gas discharge in pure  $N_2$ , pure  $H_2$  and pure He calculated from Equation (3-10) is shown in Figure 13. This equation only considers the ionization potential of the gas in determining the electron energy.

The source of electrons in a glow discharge is from ionization of the component gases and from secondary emission from the cathode. The energy of the electrons is controlled by elastic and inelastic collisions with the component gases. The inelastic processes are ionization and electronic excitations of all the components of the plasma, and vibrational and rotational excitations of the molecular components.

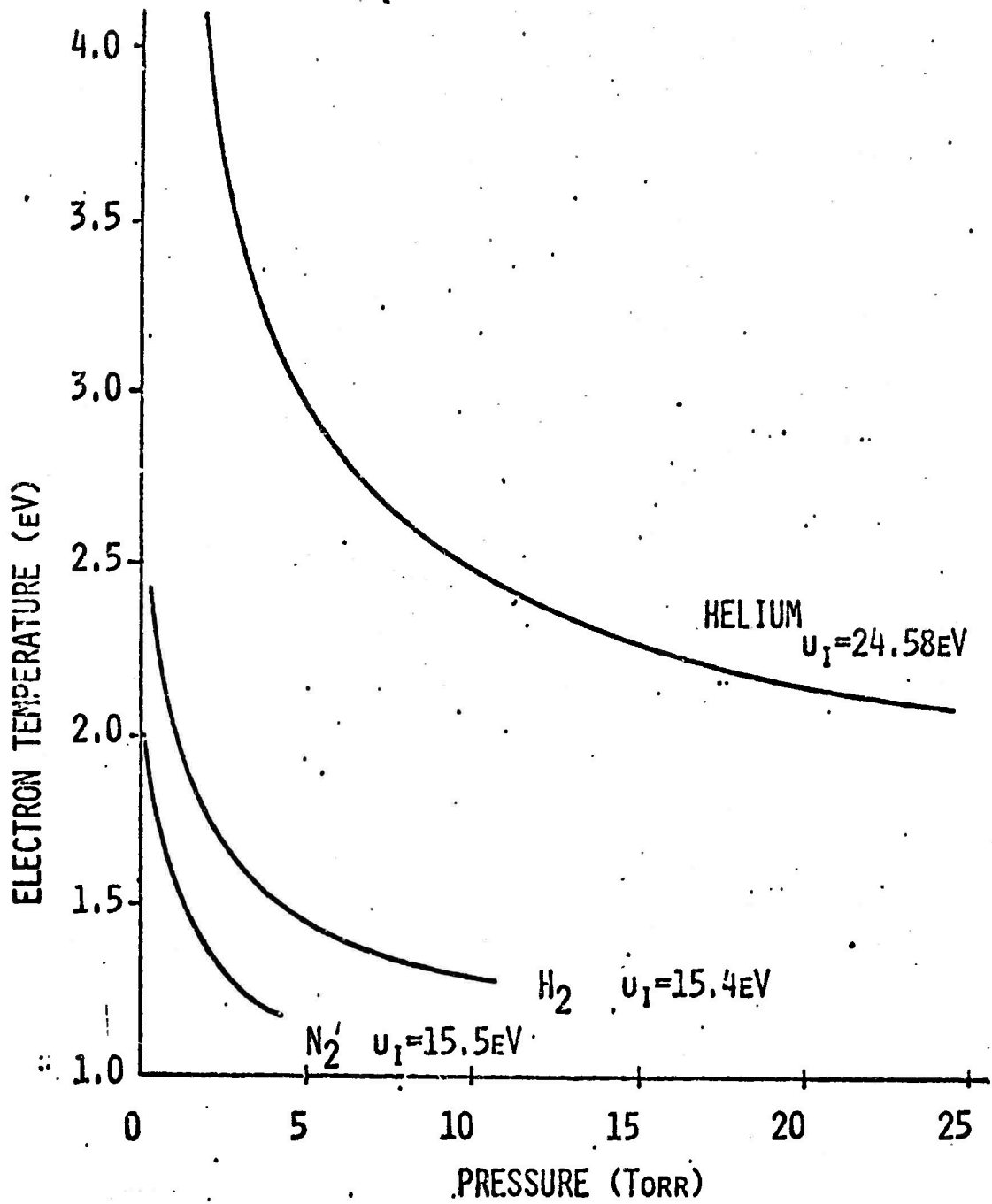


Figure 13. Electron Temperature vs. Pressure in Pure Gases

Again considering only the effect of the ionization potential, it can be shown that the electron temperature in a mixture of  $H_2$ -He can be somewhat higher than for  $H_2$  alone at the same total pressure<sup>(12)</sup>. This same argument can be applied to  $H_2$ - $C_2H_2$ -He and  $C_2H_2$ -He mixtures. This implies that high He partial pressures can be used to stabilize the discharge and still maintain high electron temperatures.

The use of pulsed excitation for  $H_2$ - $C_2H_2$ -He also increases the excitation rate through the higher current density obtainable, by at least an order of magnitude, compared to dc operation with the gas mixture used.

### 3.4 PARALLEL PUMPING EXPERIMENTS

We conducted experiments with the parallel tube shown in Figure 4 to test the hypothesis of vibrational energy transfer from excited hydrogen to acetylene. A pulsed discharge in mixtures of hydrogen and helium occurred in the side-arm or discharge region of the tube. The gases then flowed into the interaction region of the tube where they were mixed with acetylene at room temperature. In each experiment, the mirrors were aligned by filling the tube with  $N_2$ - $CO_2$ -He and adjusting for maximum average power.

A wide range of gas mixtures, flow rates, and total pressures were tried, and estimates indicate that hydrogen flow velocities up to 20 meters/sec were present. In all cases, the results were negative, and we have not observed laser emission from  $C_2H_2$  in the parallel discharge tube.

Two problems with this experiment immediately come to mind: 1) the lower level population in acetylene, and 2) vibrational deactivation by collisions with the wall. The lower level of the lasing transition is only  $729\text{cm}^{-1}$  above the ground state of acetylene. Thus, at room temperature, the population of the lower laser level is 3% to 4% of the ground state population. Larger inversions are required than for the case of  $CO_2$ , and the unpumped parts of the interaction region may be a sufficiently large fraction of the total length so that the gain cannot exceed the losses.



Diffusion coefficients have been used to estimate the lifetime of vibrationally excited  $H_2$  if wall collisions are the source of deactivation. The mutual diffusion coefficient,  $D_{12}$ , for a binary mixture of hard, elastic spheres is<sup>(22)</sup>

$$D_{12} = \frac{3}{8} \left[ \frac{\pi kT}{2M_r} \right]^{1/2} \frac{1}{\pi N d_{12}}$$

where  $M_r$  is the reduced mass  $\frac{M_1 M_2}{M_1 + M_2}$ ,

$N = N_1 + N_2$  is the total number of molecules, and

$d_{12} = \frac{d_1 + d_2}{2}$  is the average molecular diameter.

If each such collision results in a deactivation, the average lifetime of an excited specie in an infinite cylinder of radius,  $r_0$ , is

$$\tau = \frac{1}{D_{12}} \left\{ \frac{r_0}{2.405} \right\}^2$$

Table 3 shows the results of lifetime calculations using these equations. The first entry is representative of the conditions in the parallel tube which results in lifetime of 0.732msec. Thus, even at the highest estimated flow velocity for hydrogen (2.0cm/msec), the excited molecules would only travel several centimeters before a very large fraction were deactivated. In our tube, the molecules have to travel approximately 10cm to reach the interaction region, so if wall collisions are effective it is unlikely that significant numbers of vibrationally excited hydrogen are available to pump the acetylene.

The second and third entries in the table represent the conditions in the simpler, pulsed tube, and the calculations show lifetimes 3 to 4 times greater than those expected in the parallel tube. The last entry is representative

TABLE 3  
LIFETIME BY DIFFUSION TO WALLS

Pressures (Torr)			Temp (°K)	$D_{12}$ (cm <sup>2</sup> /sec)	$\tau$ (msec.)
H <sub>2</sub>	He	N <sub>2</sub>			
5	5		300	95.2	0.732
2	28		300	31.7	2.196
2	28		193	25.5	2.738
	5	5	300	40.6	1.719

$$d_{H_2} = 2.74 \text{ \AA}$$

$$d_{He} = 2.18 \text{ \AA}$$

$$d_{N_2} = 3.75 \text{ \AA}$$

$$M_{H_2} = 2.016$$

$$M_{He} = 4.002$$

$$M_{N_2} = 28.2$$

$$r_o = 0.635 \text{ cm}$$

of the situation of  $N_2$ - $CO_2$ -He in the parallel tube. Based strictly on this lifetime of 2.2msec one would come to the same conclusions reached above and predict that  $CO_2$  would not work in the parallel tube. This is obviously an erroneous conclusion as evidenced by the pulsed and CW operation reported in Section 2. Thus, some of the assumptions used in the calculation may be incorrect, at least for the  $N_2$ -He case. The Lewis-Rayleigh afterflow, which is a good indication of excited molecular nitrogen, can be seen throughout the interaction region and even some distance from the laser in the glass tubing leading to the vacuum pumps. In addition, the effectiveness of deactivating collisions with He has not been ascertained, and the small molecular weight of  $H_2$  in contrast to  $N_2$  may have important implications to the pumping process.

#### 4.0 FUTURE PLANS

In an effort to further substantiate our identification of the lasing transition, we are planning an intracavity absorption experiment. We will test the ability of normal acetylene to quench the laser, thereby determining whether or not the lasing species is, in fact, acetylene or a discharge product.

We are considering the substitution of neon for helium to see if a heavier buffer gas affects the laser performance. In addition, we hope to further define the role of hydrogen by monitoring the visible emission from discharge products both with and without the presence of  $H_2$ .

Considering the calculated lifetimes for wall deactivation, estimated flow rates, and the presence of absorption from the lower level population, the parallel pumping experiments have been discontinued until after the absorption measurements are completed. They may be taken up again later with modified equipment.

A new plasma tube will be designed, built, and tested which will minimize the regions containing unexcited gases. Other gases will be investigated with this new tube during the latter portion of the contract period.

## REFERENCES

- 1) V. P. Tychinskii, *Soviet Physics Uspekhi*, 10, 131 (1967).
- 2) C. Bradley Moore, et al, *J. Chem. Phys.*, 46, 4222 (1967).
- 3) C. J. Chen, APS Div. of Electron and Atomic Phys., New York Cith, Paper Cii (November 1969).
- 4) N. N. Sobolev and V. V. Sokovikov, *Soviet Physics Usphekhi*, 10, 153 (1967).
- 5) W. B. McKnight, *J. of Appl. Phys.*, 40, 2810 (1969).
- 6) F. Legay, et al, *Compt. Rend.*, 260, 3339 (1965).
- 7) G. Moeller and J. D. Rigden, *Appl. Phys. Letters*, 7, 274 (1965).
- 8) C. K. N. Patel, et al, *Appl. Phys. Letters*, 7, 290 (1965).
- 9) C. K. N. Patel, SPIE Laser Technology Conference, Rochester, N. Y. (Nov. 1969).
- 10) C. K. N. Patel, *Phys. Rev. Letters*, 13, 617 (1964).
- 11) S. C. Brown, Introduction to Electrical Discharges in Gases, John Wiley & Sons (1966).
- 12) C. F. Shelton, "Vibrational Energy Transfer in Gases Leading to Laser Emission", PhD Thesis, Catholic University of America (1970).
- 13) C. F. Shelton and F. T. Byrne, *Appl. Phys. Letters*, 17, 436 (1970).
- 14) G. Herzberg, Molecular Spectra and Molecular Structure, Vol. II, Infrared and Raman Spectra of Polyatomic Molecules, D. Van Nostrand Company, Inc. (1945).
- 15) F. L. Keller, "An Evaluation of the Harmonic and Anharmonic Constants of  $C_2H_2$  from a Reinvestigation of its Infrared Spectrum", PhD Thesis, University of Tennessee (1956).
- 16) R. F. Heidner and J. V. V. Kasper, *J. Chem. Phys.*, 51, 4163(1969).
- 17) F. Kaufman and J. R. Keiso, *J. Chem. Phys.*, 28, 510 (1958).
- 18) F. DeMartini and J. Ducuing, *Phys. Rev. Letters*, 17, 117 (1966).
- 19) G. J. Schulz, *Phys. Rev.*, 135, A988 (1964).
- 20) A. W. Ali and A. D. Anderson, NRL Report No. 6789, "Rate Coefficient Relevant to the  $H_2$  UV Laser" (1969).

- 21) A. von Engel, Ionized Gases, Oxford Press (1965).
- 22) E. W. McDaniel, Collision Phenomena in Ionized Gases, John Wiley & Sons, Inc. (1964).
- 23) W. A. Lathan, et al, Chem. Phys. Letters, 3, 579 (1969).
- 24) E. E. Bell and H. H. Nielsen, J. of Chem. Phys., 18, 1382 (1950)
- 25) E. E. Bell and H. H. Nielsen, J. of Chem. Phys., 19, 136 (1951).